462–469 Nucleic Acids Research, 1999, Vol. 27, No. 2

A key role for replication factor C in DNA replication checkpoint function in fission yeast

Nicola Reynolds, Peter A. Fantes and Stuart A. MacNeill*

Institute of Cell and Molecular Biology, University of Edinburgh, King's Buildings, Mayfield Road, Edinburgh EH9 3JR, UK

Received October 8, 1998; Revised and Accepted November 13, 1998

ABSTRACT

Replication factor C (RF-C) is a five subunit DNA polymerase (Pol) δ/ε accessory factor required at the replication fork for loading the essential processivity factor PCNA onto the 3′-ends of nascent DNA strands. Here we describe the genetic analysis of the *rfc2*$^+$ gene of the fission yeast *Schizosaccharomyces pombe* encoding a structural homologue of the budding yeast Rfc2p and human hRFC37 proteins. Deletion of the *rfc2*$^+$ gene from the chromosome is lethal but does not result in the checkpoint-dependent cell cycle arrest seen in cells deleted for the gene encoding PCNA or for those genes encoding subunits of either Pol δ or Pol ε. Instead, *rfc2*Δ cells proceed into mitosis with incompletely replicated DNA, indicating that the DNA replication checkpoint is inactive under these conditions. Taken together with recent results, these observations suggest a simple model in which assembly of the RF-C complex onto the 3′-end of the nascent RNA–DNA primer is the last step required for the establishment of a checkpoint-competent state.

INTRODUCTION

Replication factor C (RF-C, previously also known as activator-1) is a five subunit auxiliary factor for DNA polymerases (Pol) δ and ε that was first identified on the basis of its requirement for the replication of SV40 viral DNA *in vitro* by mammalian cell proteins (1,2). In the presence of ATP, RF-C recognises and binds to the 3′-end of primers synthesised by the Pol α–primase complex and through ATP hydrolysis facilitates the loading of the trimeric processivity factor PCNA onto DNA. Subsequently either Pol δ or Pol ε is loaded onto the DNA template, thus permitting highly processive DNA synthesis (3,4).

RF-C has been purified from a number of sources, including various mammalian cells (2,5–7) and the yeasts *Saccharomyces cerevisiae* (8–10) and *Schizosaccharomyces pombe* (11). In each case the RF-C complex comprises one large (95–130 kDa) and four small (35–40 kDa) subunits. All five proteins are related to one another at the primary sequence level. The large subunit interacts directly with PCNA and with DNA (12,13) and one or more of the small subunits are also likely to contact PCNA (7,14,15). Each subunit is essential for growth and division in budding yeast (16–18), as is the putative Rfc4 protein in *Drosophila* (19), indicating that although the individual subunits are structurally related to one another, presumably as a result of being descended from a common ancestor, their functions are not interchangeable.

Although RF-C is specifically a eukaryotic replication factor, the function it performs appears to be universally conserved. A structurally related complex in *Escherichia coli* (the γ complex) acts to load the PCNA-like β sliding clamp onto DNA for processive synthesis of chromosomal DNA by Pol III, while phage T4 DNA replication relies upon the RF-C-like gp44/62 complex loading the gp45 processivity factor (akin to PCNA) onto DNA (reviewed in 4). In addition, putative RF-C and PCNA homologues have recently been identified in archeal species (20).

In addition to being required for successful DNA replication, two of the five subunits of *S.cerevisiae* RF-C have also been shown to be required for DNA replication checkpoint function (21–23). In the absence of complete DNA replication or when DNA is damaged, checkpoints are activated that prevent entry into mitosis until replication is completed and/or the damaged DNA is repaired (24). In the yeasts *S.cerevisiae* and *S.pombe* this phenomenon is most clearly seen either when cells are treated with the DNA replication inhibitor hydroxyurea, which acts by blocking nucleotide precursor synthesis catalysed by ribonucleotide reductase, or when certain DNA replication functions are inactivated by mutation. Under these circumstances, cell cycle progression is halted, with the result that the cells accumulate in interphase and do not enter mitosis (reviewed in 25). Analysis of temperature-sensitive budding yeast mutants *rfc5-5* and *rfc2-1*, however, has shown that although DNA replication is blocked when these cells are shifted to the restrictive temperature, entry into mitosis is not inhibited, indicating that the DNA replication checkpoint is non-functional (21,23). This has led to the conclusion that RF-C function is required for both DNA replication and for DNA replication checkpoint function in budding yeast.

In the fission yeast *S.pombe* several proteins have been identified that, like Rfc2 and Rfc5 in *S.cerevisiae*, are required both for DNA replication and for replication checkpoint function. These include the origin recognition complex (ORC) components Orp1/Cdc30 and Orp2, the regulatory proteins Cdc18 and Hsk1 and the catalytic subunit of Pol α, Pol1 (26–31). Cells carrying deletions of any of these genes fail to complete DNA replication satisfactorily yet are still able to enter mitosis. This is in sharp

*To whom correspondence should be addressed. Tel: +44 131 650 7088; Fax: +44 131 650 8650; Email: s.a.macneill@edinburgh.ac.uk

contrast to the behaviour of cells carrying deletions of any of the genes encoding the essential subunits of Pol δ (Pol3/Cdc6, Cdc1 and Cdc27), the catalytic subunit of Pol ε (Cdc20/Pol2) or PCNA (Pcn1) (32–36). Deletion of any of the latter genes leads to cell cycle arrest prior to entry into mitosis, indicating that checkpoint function is not compromised by loss of any of these functions.

In order to understand better the function of the RF-C complex in DNA replication and checkpoint control, we have embarked upon a study of the cellular roles of the RF-C complex in the fission yeast *S.pombe*. Here we describe our initial genetic analysis of the *rfc2*$^+$ gene which encodes a protein related to the budding yeast Rfc2p and human hRFC37 proteins (16,18,23). Deletion of *rfc2*$^+$ from the chromosome is lethal; in marked contrast to the cell cycle arrest phenotype seen with *pol3*Δ, *cdc1*Δ or *pcn1*Δ cells (32–34), *rfc2*Δ cells proceed into mitosis with incompletely replicated DNA, indicating that *rfc2*$^+$ in fission yeast is required for DNA replication checkpoint function as well as for DNA replication itself. These results suggest a simple model in which primer recognition by RF-C is the last step required during replication fork maturation for establishment of a checkpoint-competent state.

MATERIALS AND METHODS

Yeast strains and methods

All the *S.pombe* strains used in this study have been described previously, except where indicated. For deletion of the *rfc2*$^+$ gene the sporulating diploid *leu1-32*/*leu1-32 ura4-D18*/*ura4-D18 ade6-M210*/*ade6-M216* h$^-$/h$^+$ was used (37). The wild-type control used in the spore germination experiments was *leu1-32*/*leu1-32 ura4*$^+$/*ura4-D18 ade6-M210*/*ade6-M216* h$^-$/h$^+$. Transformation of *S.pombe* was achieved by electroporation (38). Tetrad analysis was performed using a Singer micromanipulator.

Molecular cloning

Standard molecular cloning methods (39) were used throughout, except where indicated. DNA sequencing was performed using the ABI PRISM sequencing kit; samples were run on an ABI 377 sequencer. *In vitro* mutagenesis was carried out using either the Mutagene *In Vitro* Mutagenesis kit (Bio-Rad) or the Altered Sites kit (Promega) as indicated. Restriction and modification enzymes were purchased from New England Biolabs, Boehringer Mannheim or Promega and used according to the manufacturers' instructions. Oligonucleotides for sequencing and mutagenesis were synthesised by Applied Biosystems.

Analysis of *rfc2*$^+$ cDNA

To confirm that the predicted intron in the *rfc2*$^+$ gene was spliced, a partial *rfc2*$^+$ cDNA was amplified from an *S.pombe* cDNA library (40) by PCR with primers flanking the putative splice donor and acceptor sites (oligonucleotide sequences, 5′→3′: 1, ATGTCTTTCTTTGCTCCA; 2, CACACAACTGAAATAGAA) and the amplification product cloned into pGEM-T* (Promega) and sequenced using primers located within the vector sequences. The cDNA sequence was consistent with the splicing of a 52 base intron from the *rfc2*$^+$ transcript, as predicted. Subsequent cloning and sequencing of a full-length *rfc2*$^+$ cDNA confirmed that the ORF was interrupted by this intron only (not shown).

Subcloning of *rfc2*$^+$

The *rfc2*$^+$ gene is located on cosmid SPAC23D3 at nucleotide positions 1668–2742. To allow convenient manipulation of the *rfc2*$^+$ gene, a 3.8 kb *Msc*I–*Hin*dIII fragment (nt 402–4242 inclusive) encompassing the entire *rfc2*$^+$ ORF was sub-cloned into pTZ19R (Pharmacia) using the *Sma*I and *Hin*dIII sites in this vector, to make plasmid pTZ19R-Rfc2.

For expression in *S.pombe* the *rfc2*$^+$ ORF was cloned into pREP3X to make pREP3X-Rfc2 by the following method. First, the *Xba*I site located beyond the 3′-end of the *rfc2*$^+$ ORF in pTZ19R-Rfc2 was mutated to a *Sma*I site by oligonucleotide-directed *in vitro* mutagenesis, using the MutaGene kit (Bio-Rad) according to the manufacturer's instructions, to make plasmid pTZ19R-Rfc2Sma (oligonucleotide: 5′-GTTTACCACTAAACTCCCGGGGTTATGTTTAAATGT-3′, *Sma*I site underlined). Next the *rfc2*$^+$ ORF was excised from this plasmid (*Eco*RV–*Sma*I fragment) and transferred into *Sma*I-digested pREP3X, to make pREP3X-Rfc2. An intron-less form of *rfc2*$^+$ was created by *in vitro* mutagenesis of pTZ19R-Rfc2Sma (oligonucleotide: 5′-TCCAATGTCTTGGGACGATAAAGCTCAACCCAAGGT-3′). The artificial cDNA was then cloned into pREP3X (*Eco*RV–*Sma*I fragment, as above) to create plasmid pREP3X-Rfc2c. The function of this was tested by transformation into the *rfc2*$^+$/*rfc2*Δ diploid described below.

Deletion of *rfc2*$^+$

To delete the *rfc2*$^+$ gene, a 1.2 kb *Eco*RV–*Xba*I fragment encompassing the entire *rfc2*$^+$ ORF (Fig. 1) was excised from plasmid pTZ19R-Rfc2 and replaced with a *Bam*HI adapter by ligation of an oligonucleotide duplex (oligonucleotide sequences, 5′→3′: 1, CTGGATCC; 2, CTAGGGATCCAG) to make plasmid pTZ19R-Rfc2ΔB. Next the 1.8 kb *Bam*HI *ura4*$^+$ fragment from plasmid pON163 (41) was ligated into this unique *Bam*HI site to make plasmid pTZ19R-Rfc2ΔBU. The 4.4 kb *Eco*RI–*Hin*dIII fragment from this plasmid, comprising the flanking regions of the *rfc2*$^+$ gene separated by the *ura4*$^+$ selectable marker, was then used to transform a *leu1-32*/*leu1-32 ura4-D18*/*ura4-D18 ade6-M210*/*ade6-M216* h$^-$/h$^+$ strain and ura$^+$ transformants selected on EMM medium supplemented with leucine. Five stable ura$^+$ isolates were chosen for further analysis. Chromosomal DNA was prepared from these by standard methods, digested with *Hin*dIII and *Eco*RI, subjected to agarose gel electrophoresis and then blotted onto GeneScreen Plus (NEN) according to the manufacturer's instructions. The membrane was then probed using an *rfc2*$^+$ probe (linearised pTZ19R-Rfc2 labelled with [α-^{32}P]dCTP using the Boehringer Mannheim HiPrime kit according to the manufacturer's instructions). Three of the five diploids analysed by this method displayed hybridisation patterns entirely consistent with deletion of the *rfc2*$^+$ gene from one chromosome; this was confirmed by probing the same blot, after stripping of the first probe, with the *Eco*RV–*Xba*I *rfc2*$^+$ ORF fragment from pTZ19R-Rfc2 (data not shown).

Analysis of *rfc2*Δ cells

One of the five *rfc2*$^+$/*rfc2*::*ura4*$^+$ diploids identified by Southern blotting was chosen for further analysis. Following sporulation on malt extract medium, asci from this strain were dissected on yeast extract plates (supplemented with adenine and uracil) using a micromanipulator (Singer). Each ascus gave rise to two viable

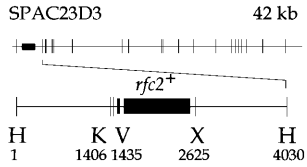

Figure 1. The *rfc2*$^+$ gene region. (Upper) Map of cosmid SPAC23D3 (EMBL accession no. Z64354) showing positions of *Hin*dIII sites (vertical bars). SPAC23D3 is 42097 bp long; the *rfc2*$^+$ gene spans nt 1668–2742, the two black boxes corresponding to exons 1 and 2. (Lower) The *rfc2*$^+$ gene (ORF indicated by a black box) is located on a 4030 bp *Hin*dIII fragment. Enzymes: H, *Hin*dIII; K, *Kpn*I; V, *Eco*RV; X, *Xba*I.

(ura$^-$) and two inviable (by implication, ura$^+$) products, indicating that *rfc2*$^+$ is an essential gene. The *rfc2*Δ spores were capable of germination and three to four divisions but arrested growth with 10–20 cells/microcolony.

For analysis of the *rfc2*Δ phenotype in liquid culture, spores were prepared from the *rfc2*$^+$/*rfc2*::*ura4*$^+$ *leu1-32/leu1-32 ura4*$^+$/*ura4-D18 ade6-M210/ade6-M216* h$^-$/h$^+$ and *leu1-32/leu1-32 ura4*$^+$/*ura4-D18 ade6-M210/ade6-M216* h$^-$/h$^+$ diploid strains in parallel. Following inoculation of the spores (to an $OD_{600\ nm}$ of 0.15) into EMM medium supplemented with leucine and adenine and growth at 30°C, samples were taken for cell number determination, flow cytometry and DAPI staining according to previously published methods (42).

Construction and analysis of a *cdc27*Δ *rfc2*Δ strain

The 4.4 kb *rfc2*::*ura4*$^+$ fragment from pTZ19R-Rfc2-ΔBU described above was transformed into a *cdc27*$^+$/*cdc27*::*his7*$^+$ *leu1-32/leu1-32 ura4-D18/ura4-D18 ade6-M210/ade6-M216 his7-366/his7-366* h$^-$/h$^+$ diploid strain (S.A.MacNeill, unpublished results) and transformants obtained on EMM plates supplemented with leucine. Thirteen stable isolates were analysed, six of which were analysed by Southern blotting of *Hin*dIII-digested chromosomal DNA (as above). Three of these were found to have deleted the *rfc2*$^+$ gene. One *cdc27*$^+$/*cdc27*::*his7*$^+$ *rfc2*$^+$/*rfc2*::*ura4*$^+$ *leu1-32/leu1-32 ura4-D18/ura4-D18 ade6-M210/ade6-M216 his7-366/his7-366* h$^-$/h$^+$ strain was analysed by tetrad dissection following sporulation on malt extract medium. For analysis in liquid culture (as above) spores were inoculated into EMM medium supplemented with leucine and adenine and grown at 30°C, with samples taken every hour for cell number determination, flow cytometry and DAPI staining according to previously published methods (42).

Construction and analysis of *rfc2* mutants

Six mutant alleles of *rfc2*$^+$ were constructed by site-directed mutagenesis of the *rfc2*$^+$ ORF. To achieve this the intron-less *rfc2*$^+$ ORF (*Xho*I–*Sma*I fragment from plasmid pTZ19R-Rfc2c) was cloned into *Sal*I- and *Sma*I-digested pALTER1 (Promega). Oligonucleotides (mutated codon underlined): 012, CTTGCTACAGCGAGCGCTAAGAGGATC, mutates Ser172→Ala; 013, ATACTTGCTACATTTACTGCTAAGAGG, Arg173→Lys; 014, CATAGAATCTGCTTGATCCAAAATTAT, Glu131→Gln; 015, AGTACCAGGAGATACATAAAACAACAT, Gly59→Val; 016, TAGAATGGTTGAATTCTTTCCAGTACC, Thr66→Asn; 017, CTGAGTCATAGAGTGTGCCTCATCCAA, Asp133→His. Each mutant allele was then sub-cloned into pREP3X (*Eco*RV–*Sma*I *rfc2* fragment into *Sma*I-digested pREP3X, as described above for construction of pREP3X-Rfc2c) for expression in *S.pombe*. For this purpose each mutant was transformed into the *rfc2*$^+$/*rfc2*::*ura4*$^+$ diploid described above and transformants obtained on EMM medium containing 5 μg/ml thiamine (to repress expression from the nmt1 promoter in pREP3X). Following sporulation on malt extract plates, spores were plated onto EMM medium supplemented with adenine with/without uracil and thiamine and incubated at 30°C for several days. Putative *rfc2*::*ura4*$^+$ (pREP3X-Rfc2) haploid colonies on EMM adenine plates were picked and analysed further to confirm their genotype.

RESULTS

rfc2$^+$: chromosomal position, gene structure and relatedness to yeast Rfc2 and human hRFC37 proteins

The *rfc2*$^+$ gene was identified during the sequencing of *S.pombe* chromosome I at the Sanger Center (Cambridge, UK) on cosmid SPAC23D3 (EMBL accession no. Z63354). The gene is located at nt 1668–2742. Figure 1 shows the structure of the *rfc2*$^+$ gene region. A single 52 bp intron was predicted in this region, encompassing nt 1742–1793; confirmation that this intron is spliced was obtained by sequencing the corresponding region of an *rfc2*$^+$ cDNA. The spliced ORF, which is fully functional *in vivo* (Materials and Methods), encodes a protein of 340 amino acids that is 53% identical to both the budding yeast Rfc2p and human hRFC37 proteins (Fig. 2A). Database searches identified an additional member of the Rfc2 sub-family (Fig. 2B) from the nematode worm *Caenorhabditis elegans*. CeRfc2 is 37% identical to SpRfc2. All seven conserved protein sequence motifs found in the small RF-C subunits are present in fission yeast Rfc2 (18). Rfc2 is also distantly related to the fission yeast Rad17 protein (43) and its budding yeast homologue Rad24p (Discussion).

Deletion of *rfc2*$^+$

In order to investigate the effects of inactivating *rfc2*$^+$, we constructed an *rfc2*$^+$/*rfc2*::*ura4*$^+$ diploid strain using the one-step gene disruption method (44; Materials and Methods). This strain, in which the entire *rfc2*$^+$ ORF was deleted from one chromosome, was then sporulated and tetrads dissected using a micromanipulator. In all 14 *rfc2*$^+$/*rfc2*::*ura4*$^+$-derived tetrads were analysed. In each case only *rfc2*$^+$ (ura$^-$) spore products were viable. Microscopic examination showed that the inviable *rfc2*Δ (ura$^+$) spores were capable of germination but arrested growth as microcolonies of 10–20 small cells.

To confirm that this phenotype was due solely to the loss of *rfc2*$^+$ function we transformed the *rfc2*$^+$/*rfc2*::*ura4*$^+$ diploid strain with plasmid pREP3X-Rfc2, which contains the *rfc2*$^+$ ORF downstream of the thiamine-repressible nmt1 promoter (Materials and Methods). Transformant colonies were sporulated and the spores plated onto EMM medium supplemented with adenine with or without thiamine to select for haploid *rfc2*Δ (pREP3X-Rfc2) isolates. Numerous such haploid isolates were identified by this procedure, irrespective of the presence or absence of thiamine in the medium. (Note that there is a low constitutive level of transcription from the nmt1 promoter even in the presence of thiamine.) This indicates that that the lethality observed was due solely to loss of *rfc2*$^+$ function.

Figure 2. (**A**) Protein sequence alignment of *S.pombe* Rfc2 (Swissprot accession no. Q09843), human hRFC37 (P35249) and *S.cerevisiae* Rfc2p (P40348). Identical residues are shaded. (**B**) Phylogenetic analysis of the small RF-C subunits. Included alongside *S.pombe* Rfc2 are the four small subunits from both budding yeast and human cells, together with *C.elegans* Rfc5 and Rfc2 homologues and *Drosophila* (19) and chicken Rfc4 homologues. Sequence alignment and phylogenetic tree construction was performed using PILEUP, DISTANCES and GROWTREE, parts of the Wisconsin Package v.9.1 (Genetics Computer Group, Madison, WI).

To examine the phenotype of *rfc2*Δ cells in greater detail, large scale spore preparations were obtained by sporulating the *rfc2*$^+$/*rfc2*::*ura4*$^+$ diploid strain in liquid culture (42). Spores were then inoculated into EMM medium lacking uracil, which only allows germination of spores carrying the *rfc2*Δ allele, which are prototrophic for uracil, and incubated at 30°C (Materials and Methods). As a control, spores prepared from a *rfc2*$^+$/*rfc2*$^+$ diploid strain heterozygous for *ura4* (i.e. *ura4*$^+$/*ura4-D18*) were processed in parallel. Hourly samples were taken from both cultures (beginning 4 h after inoculation into minimal medium) and either stained with propidium iodide and subjected to flow cytometric analysis to determine DNA content or stained with DAPI and examined by fluorescence microscopy to follow the behaviour of the nuclear material (Materials and Methods). The cell number of each culture was determined at hourly intervals.

In the control culture (*rfc2*$^+$/*rfc2*$^+$) the cell number remained constant until 12–14 h after inoculation into fresh medium and increased exponentially thereafter (Fig. 3A). DNA replication in this culture was initiated 8–10 h post-inoculation and was effectively complete (>90% of cells with a 2C DNA content) by 16 h (Fig. 3B and data not shown). At later time points (up to 24 h) only the 2C peak typical of exponentially growing *S.pombe* cells was seen (42).

Cell number in the *rfc2*$^+$/*rfc2*::*ura4*$^+$ culture began to increase ~14 h after inoculation into fresh medium and over the next 8–10 h the rate of cell number increase paralleled that seen with the control culture (Fig. 3A). At 20–22 h post-inoculation, however, the rate of increase began to slow with the result that over the period 26–32 h cell number increased by <20% (compared with a >5-fold increase in the wild-type culture over the same period). The first round of DNA replication in the *rfc2*$^+$/*rfc2*::*ura4*$^+$ culture was initiated 8–10 h after re-inoculation and was ~80% complete by 16 h (Fig. 3B and data not shown), suggesting that sufficient RF-C was carried over from the parental diploid to support at least one round of replication in the *rfc2*Δ cells. However, by 20 h after inoculation, a large fraction of the population had a ≤2C DNA content, indicating that *rfc2*Δ cells are defective in DNA replication. Cells with <1C DNA content were also detected in the 28 and 32 h samples, suggestive of an unequal division of genetic material between daughter cells. No cells with <2C DNA content are seen in the wild-type culture at these time points (legend to Fig. 3). By 24 h after inoculation, microscopic examination of the *rfc2*Δ cells stained with DAPI revealed the presence of significant numbers of cells displaying nuclear abnormalities in the *rfc2*Δ samples (Fig. 3C and D). Two aberrant phenotypes were seen, making up ~10% of the total population: cells in which the septum appeared to have cleaved the nucleus in two (cut phenotype, ~3%) and anucleate cells (~7%). By 30 h, this figure had risen to 23% (Fig. 3D).

To ask whether this phenotype was confined to the cell cycles immediately after spore germination we performed a plasmid loss experiment. Haploid *rfc2*::*ura4*$^+$ (pREP3X–Rfc2) colonies were transferred to non-selective conditions (EMM medium supplemented with leucine, adenine and thiamine) to allow loss of the plasmid and examined by DAPI staining after 48 h growth at 30°C. Similar phenotypes to those observed following *rfc2*Δ spore germination were seen in ~10% of cells at this time point, indicating that loss of checkpoint control is not confined merely to the early cell cycles following spore germination.

rfc2$^+$ is required for cell cycle arrest of *cdc27*Δ cells

The results described above indicate that the DNA replication checkpoint is not activated in *rfc2*Δ cells. However, they do not address the issue of whether the checkpoint can still be activated in *rfc2*Δ cells if DNA replication is blocked in some other way. To investigate this we tested the effects of combining the *rfc2*Δ allele with a *cdc27*Δ allele. *cdc27*$^+$ encodes the essential 54 kDa subunit of the DNA polymerase δ complex in fission yeast (11,33). As noted in the Introduction, *cdc27*$^+$ is not required for checkpoint function; *cdc27*Δ cells undergo checkpoint-mediated cell cycle arrest following spore germination, as do *pol3*Δ and *cdc1*Δ cells (32,33).

We constructed a *cdc27*$^+$/*cdc27*::*his7*$^+$ *rfc2*$^+$/*rfc2*::*ura4*$^+$ diploid strain (Materials and Methods) and analysed meiotic products, initially by tetrad dissection. In total, 50 tetrads were dissected, allowing the tentative identification of 34 tetratypes and 15 ditypes (details in Table 1). The ditype tetrads fell into two classes, equivalent to the parental and non-parental ditypes arising from a conventional cross between two haploid parents. As can be seen in Table 1, the pseudo-non-parental ditypes displayed 2:2 viable:inviable products; both viable colonies were auxotrophic for uracil and histidine and therefore genotypically *cdc27*$^+$ *rfc2*$^+$.

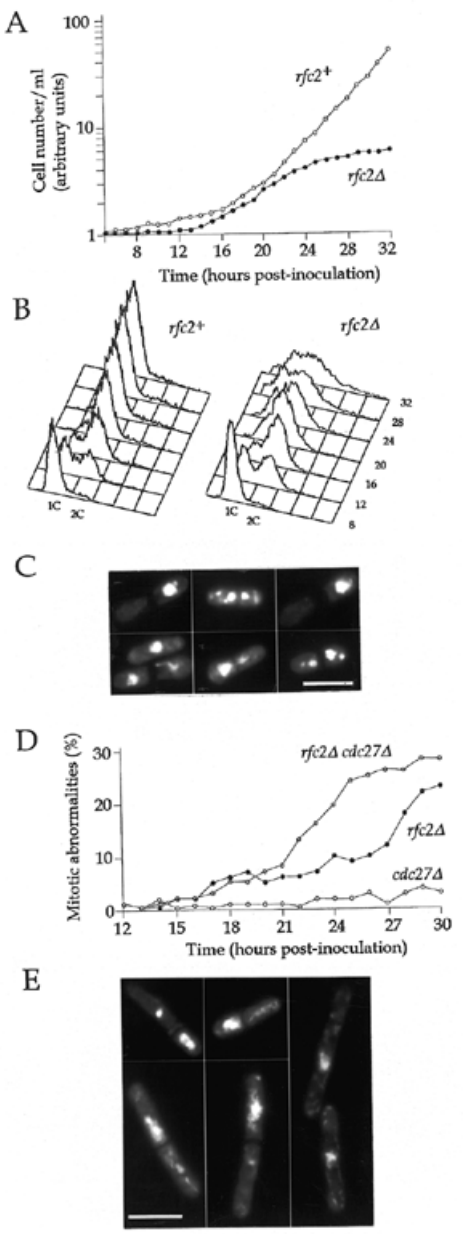

Figure 3. (**A**) Cell number (arbitrary units) per ml of culture (*y*-axis, log scale) versus time in hours (*x*-axis, linear scale) following inoculation of *rfc2*$^+$/*rfc2*$^+$ (open circles) and *rfc2*$^+$/*rfc2*Δ spores (filled circles) into supplemented minimal medium at time 0 and growth at 30°C. (**B**) Flow cytometric analysis of propidium iodide stained cells from the *rfc2*$^+$/*rfc2*$^+$ and *rfc2*$^+$/*rfc2*Δ cultures described above. The 8, 12, 16, 20, 24, 28 and 32 h time points are shown; the positions of the 1C and 2C DNA peaks are indicated. By 28 h post-inoculation a significant shoulder of cells with <1C DNA content is seen in the *rfc2*$^+$/*rfc2*Δ culture only. Note that: (i) the wild-type *rfc2*$^+$/*rfc2*$^+$ cells, like *rfc2*$^+$/*rfc2*Δ, are also heterozygous for *ura4*$^+$ (i.e. *ura4*$^+$/*ura4-D18*); (ii) following scanning, the data collected from both cultures was gated to remove ungerminated (ura$^-$) spores from the analysis on the basis of their low forward scatter. (**C**) Examples of *rfc2*Δ cells with nuclear abnormalities revealed by DAPI staining. (Upper and center) Cell division leading to unequal partitioning of the nuclear material. (Lower) Cell division leading to production of anucleate cells. Scale bar 10 µm. (**D**) Quantitation of mitotic abnormalities revealed by DAPI staining (*y*-axis, %) versus time in hours (*x*-axis) following inoculation of *rfc2*$^+$/*rfc2*Δ, *cdc27*$^+$/*cdc27*Δ and *rfc2*$^+$/*rfc2*Δ *cdc27*$^+$/*cdc27*Δ spores into supplemented minimal medium at time 0 and growth at 30°C. (**E**) Examples of *rfc2*Δ *cdc27*Δ (centre and left) and *cdc27*Δ (right) cells with/without nuclear abnormalities as revealed by DAPI staining. Scale bar 10 µm. (Details in text.)

Thus by inference the non-viable products in this class are his$^+$ ura$^+$, i.e. *cdc27*::*his7*$^+$ *rfc2*::*ura4*$^+$ double deletion haploids. Spores in this class were capable of germination and underwent several divisions before arresting as microcolonies of 10–20 predominantly small cells. Some cell elongation was observed, particularly at earlier time points, suggesting that cells may become depleted of Cdc27 before becoming depleted of Rfc2, presumably because the amounts of the two proteins carried over from the parental diploid, relative to the amounts required for DNA replication to proceed unaffected, are different. Nevertheless, the absence of significant numbers of elongated cells amongst the *rfc2*Δ *cdc27*Δ products, in contrast to the situation with *cdc27*Δ alone, where elongated cells are the predominant species (33), suggests that the *rfc2*Δ *cdc27*Δ double deletion cells are checkpoint defective, i.e. that Rfc2 is required for the cell cycle arrest seen with *cdc27*Δ cells.

Table 1. *rfc2*Δ *cdc27*Δ progeny

Progeny type	Viability	Cell size	Deduced genotype *rfc2*	*cdc27*	No. of progeny types in : TT	PD*	NPD*
1	+	Normal	+	+	1	0	2
2	-	Elongated	+	Δ	1	2	0
3	-	Normal**	Δ	+	1	2	0
4	-	Normal**	Δ	Δ	1	0	2

*The terms PD and NPD refer to ditype tetrads (parental and non-parental, respectively) equivalent to those generated in a conventional genetic cross between two haploid parents (i.e. *cdc27*Δ × *rfc2*Δ).
**Microcolonies of 10–20 normal sized cells.
TT, tetratype; PD, parental ditype; NPD, non-parental ditype.

To confirm this, we compared the properties of *cdc27*Δ *rfc2*Δ cells with *rfc2*Δ and *cdc27*Δ cells following spore germination in liquid culture. Figure 3D shows the number of abnormal mitoses observed following DAPI staining of cells from the three cultures sampled over the period 12–30 h; representative cells are show in Figure 3E.

Following spore germination *cdc27*Δ cells arrest with a single nucleus and become highly elongated (33); the number of mitotic abnormalities observed in the *cdc27*Δ culture over the period 12–22 h was ~1%, rising to 3% by 30 h (Fig. 3D). In contrast, few elongated cells were observed in the *rfc2*Δ culture, even at later time points, and the number of cells displaying mitotic abnormalities rose from ≤2% at 12–16 h to >20% at 30 h, by which time cell division in the culture had all but ceased (Fig. 3A). In the *cdc27*Δ *rfc2*Δ culture, the number of abnormal mitoses observed at 16 h was 2%, increasing slowly to 8% at 21 h, then increasing more rapidly to 28% at 30 h. Thus, 30 h post-inoculation, the number of abnormal mitotic figures in the *cdc27*Δ *rfc2*Δ double deletion was ~10 times greater than that seen with *cdc27*Δ alone, indicating that *rfc2*$^+$ function is required for the normal cell cycle arrest seen with *cdc27*Δ cells. That the proportion of abnormal mitoses increases earlier in the *cdc27*Δ *rfc2*Δ double deletion culture compared with *rfc2*Δ alone suggests that there may be an increased requirement for RF-C when Pol δ function is compromised by depletion of Cdc27.

Further evidence suggesting that *rfc2*$^+$ is required for checkpoint function came from treating *rfc2*Δ cells with the DNA synthesis inhibitor hydroxyurea. We found that the proportion of *rfc2*Δ cells

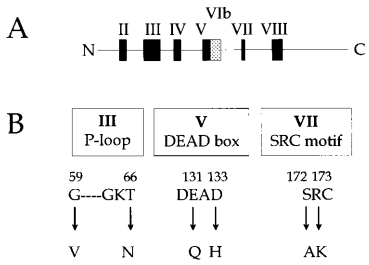

Figure 4. Sequence motifs in RF-C subunits and mutations in Rfc2. (**A**) Location of conserved sub-domains in the Rfc2 protein (18). (**B**) The mutants constructed and analysed in this study mapped to sub-domains III (G59V, T66N), V (E131Q, D133H) and VII (S172A, R173K).

displaying nuclear abnormalities at 24 h, following addition of hydroxyurea at 16 and 20 h, was undiminished at ~10%, indicating that hydroxyurea treatment cannot prevent entry into mitosis in these circumstances (data not shown).

Functional analysis of mutant Rfc2 proteins

Protein sequence alignment of the RF-C subunits identifies a number of sequence motifs that are conserved across the family (Figs 2 and 4A). These include the putative nucleotide binding site (P-loop) and the DEAD box motif. To test the importance of these residues for Rfc2 protein function we constructed two mutations (Fig. 4B) in each of the following three sub-domains: the P-loop (sub-domain III), the DEAD box (sub-domain V) and the SRC motif (sub-domain VII). Each mutant allele was cloned into plasmid pREP3X, 3′ of the regulatable nmt promoter, and the resulting plasmids transformed into the *rfc2*$^{+}$/*rfc2*::*ura4*$^{+}$ diploid strain. Transformant colonies were then sporulated and the properties of the meiotic products examined following growth on minimal medium in the presence or absence of thiamine, i.e. with the nmt promoter either repressed or derepressed (Materials and Methods). The results of this analysis are summarised in Table 2.

Table 2. *In vivo* function of Rfc2 mutants

nmt promoter :	OFF	ON
Rfc2	++	++
Rfc2-V59	–	–
Rfc2-N66	++	++
Rfc2-Q131	–	+
Rfc2-H133	–	–
Rfc2-A172	++	++
Rfc2-K173	–	+

The level of function of each of the mutant proteins is indicated as: ++, good complementation, equivalent to cells expressing wild-type Rfc2; +, growth, but poorer than that observed with cells expressing wild-type Rfc2; –, no rescued *rfc2*Δ haploids recovered.

Two of the six mutant proteins, Rfc2-N66 and Rfc2-A172, had properties that were indistinguishable from the wild-type Rfc2 protein under all conditions tested (below). The first of these, Rfc2-N66, contains a mutation in the P-loop, part of the putative nucleotide binding site of Rfc2, such that Thr66 is replaced by Asn. The corresponding mutation in several other P-loop-containing proteins such as p21^{ras}, eIF4A and the splicing factor Prp2 confer dominant negative properties on the mutant proteins (45) but no such phenotype was observed with Rfc2-N66 (even when expressed to a high level in wild-type cells; data not shown). The second mutant, Rfc2-A172, contains a mutation in the SRC motif (sub-domain VII), which is characteristic of the small RF-C subunits but which is absent in the large subunit of the human or budding yeast RF-C complexes (18). Ser172 in Rfc2 is replaced by Ala, to give the sequence ARC rather than SRC. Despite being conserved across evolution, however, it is clear that Ser172, like Thr66, is not absolutely required for Rfc2 function *in vivo*. However, it should be noted that the level of these mutant Rfc2 proteins present in cells under conditions when the nmt promoter is turned off (i.e. during growth in thiamine) may still exceed the normal level of the endogenous Rfc2 protein in wild-type cells, so that it is not possible to conclude that Rfc2-N66 and Rfc2-A172 have truly wild-type Rfc2 activity.

Two of the six mutant proteins, Rfc2-V59 and Rfc2-H133, were unable to rescue *rfc2*Δ cells even when expressed to high level (i.e. with the nmt promoter fully derepressed in the absence of thiamine). The former has Gly59 in the P-loop replaced by Val, while the latter has Asp133 in the DEAD box replaced by His (Fig. 4B). As with the mutation in the Rfc2-N66 protein, the replacement of Gly59 with Val was intended to generate a dominant negative Rfc2 protein (45), but once again no effect was seen even when Rfc2-V59 was expressed to a high level in wild-type cells.

The final two mutant proteins, Rfc2-Q131 and Rfc2-K173, could only rescue the *rfc2*Δ phenotype when expressed to a high level and even then the degree of rescue was reduced compared with that conferred by the wild-type protein. *rfc2*Δ cells rescued by either Rfc2-Q131 or Rfc2-K173 grew more slowly than cells rescued by expression of wild-type Rfc2. Microscopic examination of the rescued cells stained with DAPI (not shown) revealed the presence of a significant number of cells displaying nuclear abnormalities (~10% of the population of *rfc2*Δ cells rescued by Rfc2-Q131 and growing under selective conditions). The mitotic abnormalities seen were similar to those observed with the *rfc2*Δ deletion (i.e. anucleate and cut cells), suggesting that the checkpoint function is compromised under these conditions.

DISCUSSION

RF-C is a five subunit DNA polymerase auxiliary factor that acts as a primer recognition factor for DNA polymerases δ and ε. RF-C was first identified on the basis of its requirement for replication of SV40 viral DNA *in vitro* (2). In this system RF-C promotes the polymerase switching, from Pol α to Pol δ, which is essential for leading strand replication and for the initiation of each Okazaki fragment on the lagging strand (46). RF-C binds primers synthesised by Pol α and promotes loading of Pol δ.

In this paper we describe our initial genetic analysis of the *rfc2*$^{+}$ gene of the fission yeast *S.pombe*. *rfc2*$^{+}$ encodes a 340 amino acid protein with an equally high level of primary sequence identity (53%) to *S.cerevisiae* Rfc2 and human hRFC37 proteins (Fig. 2), suggesting that the Rfc2 protein is likely to be a component of RF-C in *S.pombe*. The *rfc2*$^{+}$ gene was identified during the sequencing of the fission yeast genome at the Sanger Centre and

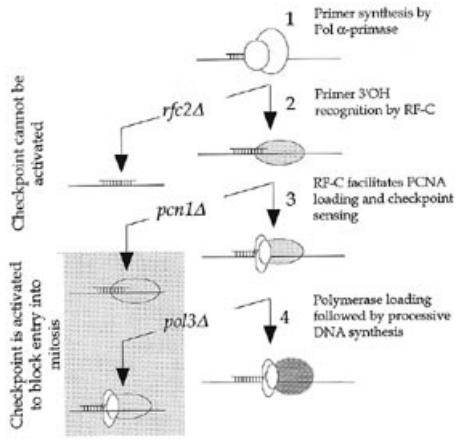

Figure 5. Temporal order of events at the replication fork following origin recognition and unwinding (polymerase switching model). Step 1, synthesis of RNA–DNA primer by Pol α–primase complex; step 2, recognition of the 3′-end of the primer by RF-C complex; step 3, ATP-dependent loading of trimeric PCNA complex onto the DNA by RF-C; step 4, PCNA-dependent loading of DNA polymerase δ or ε facilitating processive DNA synthesis extending from the primer. (Left) Effects of inhibiting steps 2–4 on DNA replication checkpoint function. Blocking steps 3 or 4 does not prevent checkpoint function; blocking steps 1 or 2, or the proceeding steps, prevents replication checkpoint sensing (Discussion).

was predicted to give rise to a spliced mRNA (Fig. 1); we have shown that the predicted intron is absent from an *rfc2*$^+$ cDNA and that an *rfc2*$^+$ gene lacking the intron is fully functional *in vivo*. The Rfc2 protein contains all the sequence motifs characteristic of RF-C subunits in general and Rfc2 sub-family members in particular (18). We have shown that mutation of certain of these conserved residues abolishes or reduces the ability of the mutant proteins to rescue an *rfc2*Δ strain, underscoring their importance for Rfc2 function (Fig. 4 and Table 2). We have deleted the *rfc2*$^+$ gene, demonstrating that *rfc2*$^+$ encodes an essential function, in common with each of the *RFC1–RFC5* genes in budding yeast (18).

Analysis of SV40 DNA replication *in vitro* has shown that, following replication origin recognition and unwinding, the pathway leading to formation of a mature, processive replication fork comprises four distinct steps in a process called polymerase switching (Fig. 5; 46). Firstly, Pol α–primase synthesises a short RNA–DNA primer (Fig. 5, step 1). Next, the 3′-OH of the primer is recognised by RF-C (step 2) which promotes the loading of PCNA onto the DNA (step 3). Following PCNA loading, DNA Pol δ is assembled onto the DNA to catalyse processive DNA synthesis (step 4). For leading strand synthesis, it is necessary for these events to occur only once at each fork, whereas for lagging strand synthesis steps 1–4 occur repeatedly to initiate synthesis of each Okazaki fragment (46).

In fission yeast it has previously been shown that inhibiting origin recognition and unwinding or any of steps 1, 3 or 4 is sufficient to inhibit DNA replication *in vivo* (25). However, the cellular consequences of preventing DNA replication by inhibiting either origin recognition and unwinding or Pol α–primase function (step 1) are very different from the consequences of preventing DNA replication by inhibiting PCNA loading (step 3) or Pol δ/Pol ε function (step 4). In the latter case, inhibition of DNA replication leads to activation of a checkpoint that prevents subsequent entry into mitosis. Thus cells deleted for one of the genes encoding Pcn1 (fission yeast PCNA) or any of the essential subunits of Pol δ or Pol ε characterised to date undergo cell cycle arrest and become highly elongated (cdc phenotype) (32–36). In contrast, inhibition of origin recognition and unwinding or Pol α–primase function (step 1) does not result in checkpoint activation; instead cells deleted for the genes encoding the ORC components Orp1 or Orp2 (27,28,47) or the single-stranded DNA binding protein Rpa1/Rad11 (48) or the catalytic subunit of Pol α, Pol1 (31), have been shown to proceed into mitosis with unreplicated DNA (cut phenotype).

In this paper we show that inhibition of RF-C function (Fig. 5, step 2) by deletion of the *rfc2*$^+$ gene results in similar behaviour to that seen with cells in which either origin recognition and unwinding or Pol α–primase function (step 1) is blocked, indicating that RF-C is required both for DNA replication and for DNA replication checkpoint function in fission yeast. This is in marked contrast to the situation reported for Pcn1 (PCNA), which although required for DNA replication is not required for replication checkpoint function (34,49). Taken together, these results imply that RF-C must have two distinct cellular functions, being required both for Pcn1 loading at the replication fork (a step that has no bearing on the function of the checkpoint, since Pcn1 itself is not required for checkpoint function; 34,49) and also for permitting checkpoint sensing. To investigate this further, we are currently screening for mutants that uncouple the two functions of Rfc2. Such mutants might be either replication-competent but checkpoint-defective (cut phenotype displayed when DNA replication blocked by, for example, hydroxyurea) or mutants that are replication-defective but checkpoint-competent (conditional lethal mutants that undergo cell cycle arrest under restrictive conditions).

Taking into consideration the temporal order of events at the replication fork outlined above and shown in Figure 5, our results suggest that RF-C loading is the last step required in this pathway in order to permit checkpoint sensing. If that were the case then the inability of cells defective in origin recognition and unwinding or Pol α–primase function to undergo checkpoint-mediated cell cycle arrest may simply reflect the fact that primer recognition by RF-C is prevented in these circumstances. This implies that the components of ORC, for example, or the ORC regulator Cdc18 need not be themselves directly involved in replication checkpoint function, contrary to previous models (50,51).

A key question be to addressed is how does RF-C function to permit the establishment of a checkpoint-competent state? In this regard it is interesting to note that the fission yeast Rad17 protein, an essential component of the checkpoint whose function is disrupted in *rfc2*Δ cells, displays limited sequence similarity to members of the RF-C family, suggesting that the two proteins have similar biochemical functions or share common interacting elements (43). Whilst Rad17 is not part of RF-C as defined biochemically, it is tempting to speculate that the function of Rad17 may be dependent upon it associating with RF-C at the replication fork, in which case either inactivation of RF-C (as occurs in *rfc2*Δ cells described here) or failure to synthesise a primer that can be recognised by RF-C (as presumably occurs in *orp1*Δ, *cdc18*Δ or *pol1*Δ cells) would result in loss of Rad17 function and disruption of the checkpoint. In support of such a model Sugimoto and co-workers (52) have recently demonstrated a physical association between the *S.cerevisiae* Rfc2 and Rfc5 proteins and the Rad17 homologue Rad24p.

ACKNOWLEDGEMENTS

We would like to thank our friends and colleagues in Edinburgh and elsewhere for their assistance during the course of this work. In particular we are are grateful to Dr K.Hentschel (RZLB, Berlin) for the *rfc2*$^{+}$ cosmid, A.Sanderson (ICAPB, University of Edinburgh) for FACScan analysis, J.Davidson for media preparation, Dr K.Sugimoto (University of Nagoya) for helpful discussions and Professor J.Beggs (ICMB, University of Edinburgh) for advice concerning DEAD box proteins. N.R. and S.M. are supported by the Wellcome Trust.

REFERENCES

1 Fairman,M.P. and Stillman,B. (1988) *EMBO J.*, **7**, 1211–1218.
2 Tsurimoto,T. and Stillman,B. (1989) *Mol. Cell. Biol.*, **9**, 609–619.
3 Stillman,B. (1994) *Cell*, **78**, 725–728.
4 Stillman,B. (1996) In DePamphilis,M.L. (ed.), *DNA Replication in Eukaryotic Cells*. Cold Spring Harbor Laboratory Press, Cold Spring Harbor, NY, pp. 435–460.
5 Lee,S.H., Kwong,A.D., Pan,Z.Q. and Hurwitz,J. (1991) *J. Biol. Chem.*, **266**, 594–602.
6 Podust,V.N., Georgaki,A., Strack,B. and Hubscher,U. (1992) *Nucleic Acids Res.*, **20**, 4159–4165.
7 Pan,Z.Q., Chen,M. and Hurwitz,J. (1993) *Proc. Natl Acad. Sci. USA*, **90**, 6–10.
8 Fien,K. and Stillman,B. (1992) *Mol. Cell. Biol.*, **12**, 155–163.
9 Yoder,B.L. and Burgers,P.M.J. (1991) *J. Biol. Chem.*, **266**, 22689–22697.
10 Burgers,P.M.J. (1991) *J. Biol. Chem.*, **266**, 22698–22706.
11 Zuo,S.J., Gibbs,E., Kelman,Z., Wang,T.S.F., O'Donnell,M., MacNeill,S.A. and Hurwitz,J. (1997) *Proc. Natl Acad. Sci. USA*, **94**, 11244–11249.
12 Fotedar,R., Mossi,R., Fitzgerald,P., Rousselle,T., Maga,G., Brickner,H., Messier,H., Kasibhatla,S., Hubscher,U. and Fotedar,A. (1996) *EMBO J.*, **15**, 4423–4433.
13 Montecucco,A., Rossi,R., Levin,D.S., Gary,R., Park,M.S., Motycka,T.A., Ciarrocchi,G., Villa,A., Biamonti,G. and Tomkinson,A.E. (1998) *EMBO J.*, **17**, 3786–3795.
14 Chen,M., Pan,Z.Q. and Hurwitz,J. (1992) *Proc. Natl Acad. Sci. USA*, **89**, 5211–5215.
15 Chen,M., Pan,Z.Q. and Hurwitz,J. (1992) *Proc. Natl Acad. Sci. USA*, **89**, 2516–2520.
16 Noskov,V., Maki,S., Kawasaki,Y., Leem,S.H., Ono,B.I., Araki,H., Pavlov,Y. and Sugino,A. (1994) *Nucleic Acids Res.*, **22**, 1527–1535.
17 Gary,S.L. and Burgers,P.M.J. (1995) *Nucleic Acids Res.*, **23**, 4986–4991.
18 Cullmann,G., Fien,K., Kobayashi,R. and Stillman,B. (1995) *Mol. Cell. Biol.*, **15**, 4661–4671.
19 Harrison,S.D., Solomon,N. and Rubin,G.M. (1995) *Genetics*, **139**, 1701–1709.
20 Edgell,D.R. and Doolittle,W.F. (1997) *Cell*, **89**, 995–998.
21 Sugimoto,K., Shimomura,T., Hashimoto,K., Araki,H., Sugino,A. and Matsumoto,K. (1996) *Proc. Natl Acad. Sci. USA*, **93**, 7048–7052.
22 Sugimoto,K., Ando,S., Shimomura,T. and Matsumoto,K. (1997) *Mol. Cell. Biol.*, **17**, 5905–5914.
23 Noskov,V.N., Araki,H. and Sugino,A. (1998) *Mol. Cell. Biol.*, **18**, 4914–4923.
24 Hartwell,L.H. and Weinert,T.A. (1989) *Science*, **246**, 629–634.
25 MacNeill,S.A. and Nurse,P. (1997) In Pringle,J.R., Broach,J.R. and Jones,E.W. (eds), *The Molecular and Cellular Biology of the Yeast Saccharomyces: Cell Cycle and Cell Biology*. Cold Spring Harbor Laboratory Press, Cold Spring Harbor, NY, Vol. 3, pp. 697–763.
26 Grallert,B. and Nurse,P. (1996) *Genes Dev.*, **10**, 2644–2654.
27 Muzi-Falconi,M. and Kelly,T.J. (1995) *Proc. Natl Acad. Sci. USA*, **92**, 12475–12479.
28 Leatherwood,J., LopezGirona,A. and Russell,P. (1996) *Nature*, **379**, 360–363.
29 Masai,H., Miyake,T. and Arai,K. (1995) *EMBO J.*, **14**, 3094–3104.
30 Kelly,T.J., Martin,G.S., Forsburg,S.L., Stephen,R.J., Russo,A. and Nurse,P. (1993) *Cell*, **74**, 371–382.
31 D'Urso,G., Grallert,B. and Nurse,P. (1995) *J. Cell Sci.*, **108**, 3109–3118.
32 Francesconi,S., Park,H. and Wang,T.S.F. (1993) *Nucleic Acids Res.*, **21**, 3821–3828.
33 MacNeill,S.A., Moreno,S., Reynolds,N., Nurse,P. and Fantes,P.A. (1996) *EMBO J.*, **15**, 4613–4628.
34 Waseem,N.H., Labib,K., Nurse,P. and Lane,D.P. (1992) *EMBO J.*, **11**, 5111–5120.
35 D'Urso,G. and Nurse,P. (1997) *Proc. Natl Acad. Sci. USA*, **94**, 12491–12496.
36 Sugino,A., Ohara,T., Sebastian,J., Nakashima,N. and Araki,H. (1998) *Genes Cells*, **3**, 99–110.
37 Moreno,S., Klar,A. and Nurse,P. (1991) *Methods Enzymol.*, **194**, 795–823.
38 Prentice,H.L. (1992) *Nucleic Acids Res.*, **20**, 621.
39 Sambrook,J., Fritsch,E.F. and Maniatas,T. (1989) *Molecular Cloning: A Laboratory Manual*, 2nd Edn. Cold Spring Harbor Laboratory Press, Cold Spring Harbor, NY.
40 Fikes,J.D., Becker,D.M., Winston,F. and Guarente,L. (1990) *Nature*, **346**, 291–294.
41 Weilguny,D., Praetorius,M., Carr,A., Egel,R. and Nielsen,O. (1991) *Gene*, **99**, 47–54.
42 MacNeill,S.A. and Fantes,P.A. (1997) *Methods Enzymol.*, **283**, 440–459.
43 Griffiths,D.J.F., Barbet,N.C., McCready,S., Lehmann,A.R. and Carr,A.M. (1995) *EMBO J.*, **14**, 5812–5823.
44 Rothstein,R.J. (1983) *Methods Enzymol.*, **101**, 202–211.
45 Pause,A., Methot,N., Svitkin,Y., Merrick,W.C. and Sonenberg,N. (1994) *EMBO J.*, **13**, 1205–1215.
46 Waga,S. and Stillman,B. (1994) *Nature*, **369**, 207–212.
47 Grallert,B. and Nurse,P. (1996) *Genes Dev.*, **10**, 2644–2654.
48 Parker,A.E., Clyne,R.K., Carr,A.M. and Kelly,T.J. (1997) *Mol. Cell. Biol.*, **17**, 2381–2390.
49 Arroyo,M.P., Downey,K.M., So,A.G. and Wang,T.S.F. (1996) *J. Biol. Chem.*, **271**, 15971–15980.
50 Kelly,T.J., Nurse,P. and Forsburg,S.L. (1993) *Cold Spring Harbor Symp. Quant. Biol.*, **58**, 637–644.
51 Nishitani,H. and Nurse,P. (1995) *Cell*, **83**, 397–405.
52 Shimomura,T., Ando,S., Matsumoto,K. and Sugimoto,K. (1998) *Mol. Cell. Biol.*, **18**, 5485–5491.